

The influence of polishing parameters on acoustic emission: Molecular dynamics study

Cite as: AIP Conference Proceedings **2167**, 020249 (2019); <https://doi.org/10.1063/1.5132116>
Published Online: 19 November 2019

A. Yu. Nikonov, and A. M. Zharmukhambetova



[View Online](#)



[Export Citation](#)

ARTICLES YOU MAY BE INTERESTED IN

[Investigation of acoustic emission produced during processing by sliding indenter: Molecular dynamics study](#)

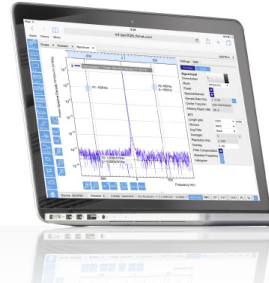
AIP Conference Proceedings **2167**, 020246 (2019); <https://doi.org/10.1063/1.5132113>

[Molecular dynamic investigation of acoustic emission during mechanical treatment](#)

AIP Conference Proceedings **2167**, 020247 (2019); <https://doi.org/10.1063/1.5132114>

[Molecular dynamics simulation of polycrystalline metal surface treatment](#)

AIP Conference Proceedings **2167**, 020248 (2019); <https://doi.org/10.1063/1.5132115>



Lock-in Amplifiers



[Watch the Video](#)

The Influence of Polishing Parameters on Acoustic Emission: Molecular Dynamics Study

A.Yu. Nikonorov^{1,2, a)} and A.M. Zharmukhametova^{1,2, b)}

¹*Institute of Strength Physics and Materials Science, SB RAS, 2/4 Akademicheskii Ave., Tomsk, 634055, Russia*

²*National Research Tomsk State University, 36 Lenin Ave., Tomsk, 634050, Russia*

^{a)}Corresponding author: anickonoff@ispms.ru
^{b)}zharmukhametova@gmail.com

Abstract. In the paper, simulation of the polishing process of copper crystal was carried out using the method of molecular dynamics. We investigated the effect of the size of the indenter on the acoustic emission in the sample. The velocity of the center of mass of the sensor, changing of the system energy and the formation of defects during loading was analyzed. According to the obtained results, an increase in the radius of curvature of the indenter leads to changes in the main mechanism of plastic deformation of the material, and hence changes in the signal AE.

INTRODUCTION

Analysis of acoustic emission (AE) is one of the most common methods for monitoring of mechanical systems. A distinctive feature of this approach is the ability to identify different structure changes by the generated acoustic signals without modifying the properties or shape of the material. The AE relates to traditional non-destructive methods of testing. At present, the use of the AE method to monitor the state of mechanical systems (gearboxes and bearing friction units) and detect vibrations is gaining popularity. This approach is also used in the manufacture of machine parts, for example, in metal cutting machinery, where AE is used to monitor the state of the cutting tool or the chip formation effect on tool state. The appearance of vibrations during processing of this kind is highly undesirable, because they lead to a decrease in the quality of the obtained parts. Analysis of AE makes it possible to detect vibrations, but it is necessary to separate signals arising both during tribological contact of the workpiece with the tool and during intensive plastic deformation of the material. It is difficult to interpret the sources of acoustic emission due to complex internal structure of polycrystalline materials and the variety of processes occurring during plastic deformation in the volume of the workpiece. Today this problem is efficiently solved using various numerical simulation methods in combination with experiment [1 – 5]. The application of molecular dynamics method will allow us to identify and investigate sound oscillations that arise during indentation in different mode. It is proposed to correlate the received acoustic emission signals with the change in the internal structure of the material and loading condition by using this approach. The aim of the present work is to study the influence of indenter size, generated structure defects and internal energy change of a sample, on AE signals during nanopolishing.

NUMERICAL MODEL

The study was conducted in the framework of molecular dynamics method using the software package LAMMPS [6, 7]. To study the processes of plastic deformation and the elastic waves that arise in the volume, an iron sample was modeled, which was a rectangular parallelepiped $40 \times 20 \times 9$ nm in size along the X, Y, and Z axes, respectively. The total number of atoms was about 400,000. A representation of the sample at the initial time is shown in Fig. 1. Along the Z-axis of the laboratory coordinate system, periodic boundary conditions were specified. Four lower and right atomic layers (marked in yellow in Fig. 1) were fixed, imitating the substrate. A special

damping layer of atoms was set between the substrate and the sample (marked in blue in Fig. 1), for which the procedure for reducing kinetic energy accumulated due to dynamic loading was used. Using this layer allowed us to simulate the energy distribution deep into the material in the direction of the X- and Y-axes. The thickness of the “damping” layer was 1 nm. The simulations were carried out for 1K temperature. The zero temperature was used to evaluate the effect of heat motion on the system dynamics. The interaction between atoms is described within the embedded atom method [8,9]. The polishing was carried out by an indenter. This indenter was a combination of a completely rigid cylinder of atoms (material indenter) with a radius of R_m (2 nm; 4 nm and 6 nm) and a field force indenter with a radius of $R_f=R_m+0.2$ nm. The axes of indenter and cylinder were coincided and oriented along the Z-axis. The material indenter prescribes adhesion properties due to the mutual attraction of atoms. The field force indenter reduced the adhesion forces between the atoms of the sample and the indenter. There were forces directed from the axis of the cylinder on the atoms of the sample inside the region of the force field indenter. The magnitude of the force is described by $F(r) = -K(r - R)^2$, where K – proportionality factor, r – distance from cylinder axis to atom and R – cylinder radius. The acting force $F(r)$ was equal to zero for atoms outside the indenter ($r > R$). The polishing simulation was carried out at the constant rate 0.1 Å/ps along the X-axis. To obtain acoustic emission signals on the free surfaces of the sample in the YOZ plane, region with dimensions of $2 \times 3 \times 9$ nm was distinguished (white fragment in Fig.1 is sensor). The velocity of the center of mass of the atoms was analyzed in this region.

The Common Neighbor Analysis and Dislocation Extraction Algorithm were used [10, 11] to analyze the changes in the structure of the modeled samples. These approaches are widely used to determine the local crystal structure of the material (bcc, fcc, hcp) and reveal various types of dislocations [12, 13].

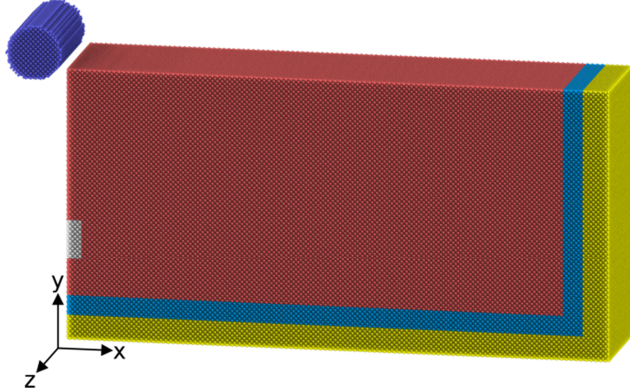


FIGURE 1. Structure of the simulated sample at initial time.

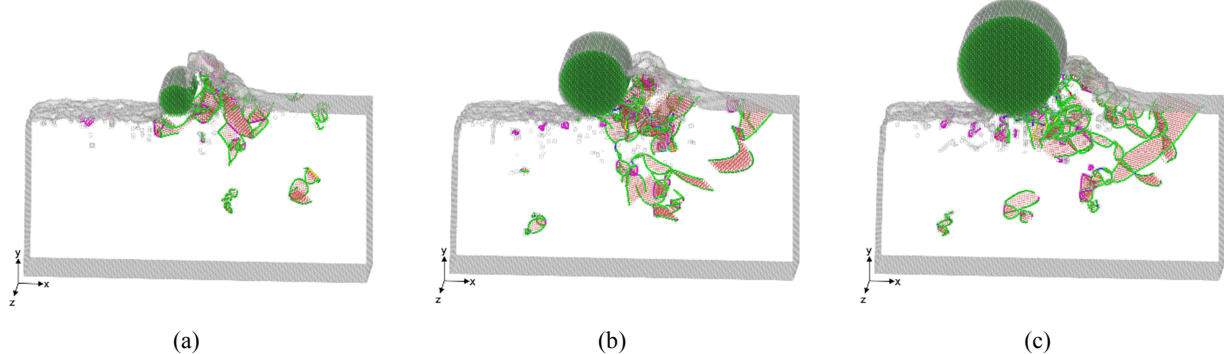


FIGURE 2. The structure of the sample at time 2.03 ns when loaded by an indenter with a radius of a) 2 nm; b) 4 nm and c) 6 nm. For better visualization of the internal structure, only atoms with a structure other than fcc are shown. The atoms with a local hcp structure are marked in red, the indenter atoms are in green. Lines show dislocations: green – $1/6 <112>$, purple – $1/6 <110>$.

SIMULATION RESULTS

The radius of curvature of the indenter was chosen as the variable parameter of the technological process. The calculations were carried out for 3 values of the indenter radius: 2 nm, 4 nm, and 6 nm with the same depth of penetration into the sample. According to the obtained results, in the process of indenter sliding, two main mechanisms of plastic deformation are realized: the formation of a “bulge” from atoms pushed aside by the indenter

(formation of chips) and the indentation of atoms of the near-surface layer into the bulk of the material. Depending on the size of the indenter, one or the other mechanism may prevail. Figure 2 shows the structure of the samples at the end of the calculations. It is seen that an increase in the radius leads to a decrease in the number of atoms pushed aside in front of the indenter and a greater change in the internal structure of the sample. It was previously shown that the redistribution of energy in a sample can affect the AE signal [14]. The greatest influence on the value of the internal energy of the system is exerted by structural defects of the crystal lattice. Therefore, using the Common Neighbor Analysis, we calculated the number of atoms in a sample with a fcc, hcp local structure and an undefined structure. Atoms with a hcp local structure are located in the planes of stacking fault and twin, atoms with an indefinite structure are usually located near dislocations, vacancies, and on free surfaces. Figure 3 shows a graph of the fraction of atoms, in which the structure differs from fcc, against the loading time of the system. From the graph it can be seen that after 0.75 ns, the movement of indenters with radii of 4 nm and 6 nm leads to the formation of a larger number of defects, as compared with the 2 nm indenter. It can be concluded that the size of the indenter affects the internal energy of the system, and, consequently, the AE signals.

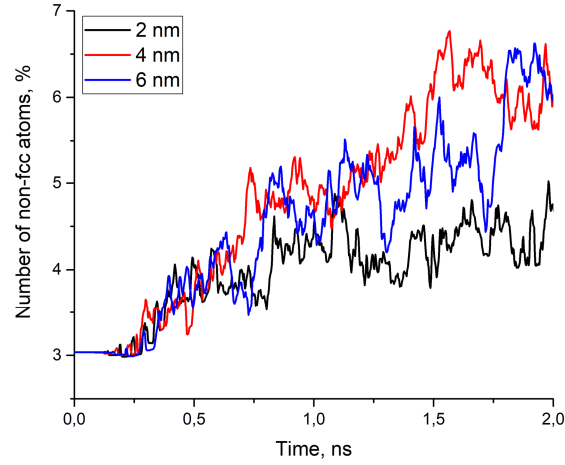


FIGURE 3. The proportion of atoms with a structure other than fcc depending on the loading time.

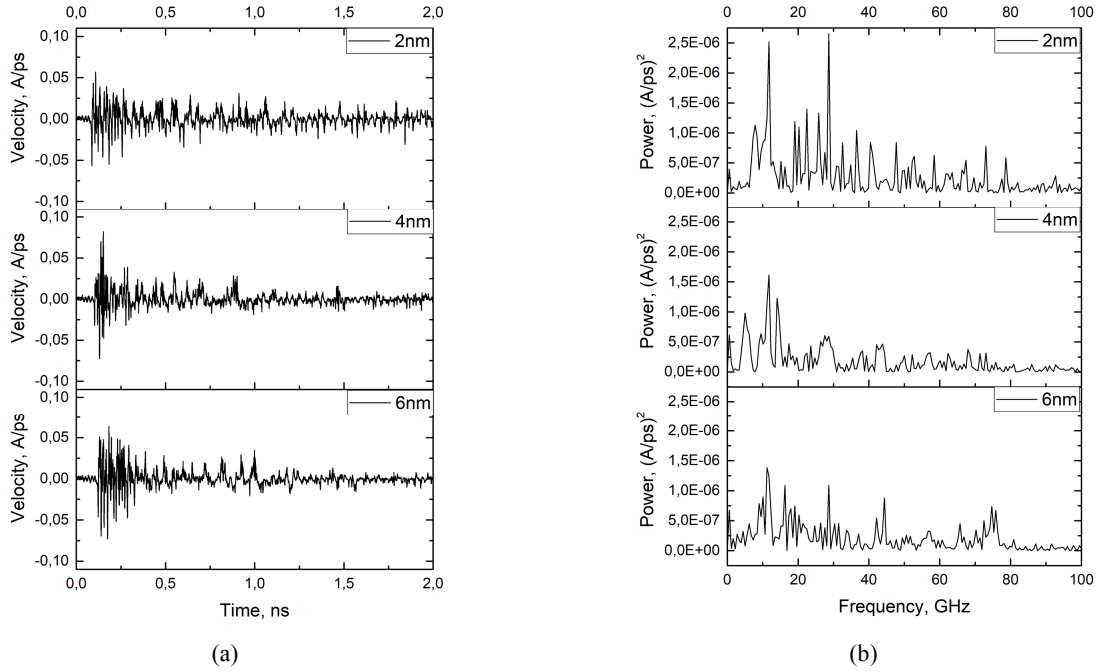


FIGURE 4. Change in sensor speed (a) and power spectral density of received signal (b).

To verify this assumption, changes in the velocity of the center of mass of the sensor as a function of time for the three test samples (Fig. 4a) were analyzed. There is a clear difference in the curves on the graphs. It is due to the processes occurring in the sample during deformation. Fourier analysis was used to study and compare signals. Figure 4b shows the power spectrum of the studied signals in the range up to 100 GHz. From the comparison of the curves it is possible to distinguish increased values of power at certain frequencies for a sample which loaded by an indenter with a radius of 2 nm compared to the others. For a sample loaded by an indenter with a radius of 6 nm, it is possible to distinguish the presence of several pronounced peaks located at frequencies of 45 and 75 GHz. For a sample with an indenter of 4 nm, these peaks are also observed, but less pronounced. It can be assumed that an increase in the indenter radius leads to the appearance of high-amplitude oscillations at some frequencies and, as noted earlier, a change in the processes of plastic deformation. Thus, from analysis of the acoustic emission signals, it is possible to determine which of the two main deformation mechanisms is realized during the processing of polishing.

CONCLUSIONS

The objective of the present work was to study the acoustic emission response to plastic deformation by indenters with different radii. The AE signal was simulated by the velocity of the center of mass of a group of atoms on the lateral face of the sample and resulted from applied forces. The results show that an increase in the size of the indenter leads to the formation of a larger number of defective configurations in the sample volume, so we have a larger amount of material involved in the deformation. I.e. the mechanism of the formation of a “bulge” from atoms pushed aside by the indenter (formation of chips) becomes less pronounced than mechanism of the indentation of atoms of the near-surface layer into the bulk of the material. In turn, this affects the AE signal. The resulting AE signal can be composed of different components that have different frequencies and amplitudes. On the basis of the analysis of changes in the AE signal, it can be assumed which of the mechanisms of plastic deformation of the material is realized in the material. The obtained results can be used to create control equipment for mechanical processing of the material.

ACKNOWLEDGMENTS

The work was carried out at the financial support of the Russian Science Foundation grant No. 17-79-10081.

REFERENCES

1. A.S. Grigoriev, E.V. Shilko, S.V. Astafurov, A.V. Dimaki, E.M. Vysotsky, and S.G. Psakhie, *Phys. Mesomech.* **19**, 136–148 (2016).
2. A.R. Shugurov, A.V. Panin, A.I. Dmitriev, and A.Yu. Nikonov, *Wear.* **408-409**, 214-221 (2018).
3. A.I. Dmitriev and W. Österle, *Tribol. Lett.* **53**, 337–351 (2014).
4. A.I. Dmitriev, A.Yu. Nikonov, A.R. Shugurov, and A.V. Panin, *Appl. Surf. Sci.* **471**, 318-327 (2019).
5. S.G. Psakhie, V.L. Popov, E.V. Shilko, A.Yu. Smolin, and A.I. Dmitriev, *Phys. Mesomech.* **12(5-6)**, 221-234 (2009).
6. S.J. Plimpton, *J. Comp. Phys.* **117**, 1–19 (1995).
7. S.G. Psakhie, K.P. Zolnikov, D.S. Kryzhevich, and A.V. Korchuganov, *Sci. Rep.* **9**, 3867 (2019).
8. Y. Mishin, M.J. Mehl, D.A. Papaconstantopoulos, A.F. Voter, and J.D. Kress, *Phys. Rev. B* **63**, 224106 (2001).
9. A.V. Korchuganov, A.N. Tyumentsev, K.P. Zolnikov, I.Yu. Litovchenko, D.S. Kryzhevich, E. Gutmanas, S. Li, Z. Wang, and S.G. Psakhie, *J. Mater. Sci. Technol.* **35**, 201-206 (2019).
10. J.D. Honeycutt, and H.C. Andersen, *J. Phys. Chem.* **91**, 4950–4963 (1987).
11. A. Stukowski, V.V Bulatov, and A. Arsenlis, *Model. Simul. Mater. Sci. Eng.* **20**, 85007 (2012).
12. K.P. Zolnikov, D.S. Kryzhevich, and A.V. Korchuganov *Lett. Mater.* **9**, 197-201 (2019).
13. K.P. Zolnikov, A.V. Korchuganov, D.S. Kryzhevich, and S.G. Psakhie, *Phys. Mesomech.* **21**, 492-497 (2018).
14. A.V. Filippov, A.Y. Nikonov, V.E. Rubtsov, A.I. Dmitriev, and S.Y. Tarasov, *J. Mater. Process. Tech.* **246**, 224-234 (2017).